DALTON

Interligand CH · · · π interaction in binary cobalt(III) complexes of *N*-pyridoxy-L-amino acids. Biological significance of the pyridoxal 2-methyl group

Koichiro Jitsukawa,*[a] Kouji Iwai,[a] Hideki Masuda,*[a] Hisanobu Ogoshi[b] and Hisahiko Einaga[a]

[a] *Department of Applied Chemistry, Faculty of Engineering, Nagoya Institute of Technology, Showa-ku, Nagoya 466, Japan*
[b] *Department of Synthetic Chemistry, Faculty of Engineering, Kyoto University, Yoshida, Sakyo-ku, Kyoto 606, Japan*

Reaction of $K_3[Co(CO_3)_3]$ with 2 equivalents of *N*-pyridoxy-L-amino acid (pyridoxy = 3-hydroxy-5-hydroxymethyl-2-methylpyridin-4-ylmethyl; amino acid = alanine, leucine, phenylglycine, phenylalanine, *p*-nitrophenylalanine, *p*-methoxyphenylalanine, or tryptophan) afforded the bis(*N*-pyridoxy-L-amino acidato)cobalt(III) complex as a single band on anion-exchange chromatography. Each complex has been isolated as its sodium salt and characterized in aqueous solution by UV/VIS circular dichroism (CD), and ^{1}H NMR spectra and by X-ray crystallographic analysis in the solid state. The cobalt(III) atom is co-ordinated to two *trans*(N)-meridional *N*-pyridoxy-L-amino acid ligands. The 2-methyl group of one pyridoxal moiety lies over the aromatic ring of another pyridoxal ring with separations of 3.67 and 3.56 Å. The ^{1}H NMR resonance of the 2-methyl group shows an upfield shift when compared with that of the free pyridoxyamino acid. The selective formation of the *trans*(N)-meridional-Λ-[*R*(*N*), *R*(*N*)] diastereoisomer is interpreted in terms of an interligand CH · · · π interaction. The CD and ^{1}H NMR spectra suggest that addition of 1 equivalent HCl weakens this interaction. The biological significance of the pyridoxy 2-methyl group in vitamin B_6 coenzyme is discussed.

Non-covalent interactions such as hydrogen bonding and electrostatic interactions are crucial for molecular recognition and catalysis in biological systems.[1–3] The side-chain groups of amino acid residues in proteins are sometimes responsible for such interactions. The interactions at the active site of a enzyme–substrate complex in a metalloenzyme can be regarded as ligand–ligand interactions around the metal atom and these play a vital role in enzyme catalysis. Examples demonstrating such multibonding interactions are carboxypeptidase A (CPA) with the model substrate glycyl-L-tryosine[4,5] and leucine aminopeptidase (LAP) with bestatin.[6,7] In the former the guanidinium group of arginine-145 of CPA and a hydrophobic pocket interact with the carboxylate and the tyrosine phenol group of the substrate, respectively, and in the latter the carboxylate group of aspartic acid-273 of LAP and a hydrophobic pocket interact with the amino and the leucine isopropyl group of the substrate, respectively, in which they fix each other in a specific way around the central zinc ion. The interactions present in them are the directional bindings and these binding energies are rather high (3–10 kcal mol^{-1}; cal = 4.184 J).[2] An appropriate orientation of these interacting groups in biological systems facilitates the reaction selectivity of substrates.

We have been studying weak interactions such as intramolecular aromatic ring stacking, electrostatic ligand–ligand interaction and hydrogen bonding, as a simple molecular recognition model for enzyme–substrate complexes, by spectroscopic, thermodynamic and X-ray diffraction methods.[8–11] On the other hand, hydrophobic interactions between aliphatic groups and between aliphatic and aromatic groups, which are rather weak in comparison with the above-mentioned interactions, are also known to occur in biological systems.[2] These interactions are considered to contribute to determining their structural conformation. An aliphatic–aromatic or more specifically a CH · · · π interaction has been recognized by some spectroscopists and X-ray crstallographers.[12–16] There are some previous reports on this sort of weak interaction. Fischer and Sigel[17] showed that the stability of ternary complexes containing an amino acid and 2,2′-bipyridine or 1,10-phenanthroline increases with an increase in the interligand interaction between aromatic and aliphatic groups. Okawa[13] also suggested the presence of a CH · · · π interaction through a synthetic study on bi- and tri-valent metal complexes of 1-L-menthoxy-3-benzoylacetone, although this work gives no direct evidence of such an interaction. Recently, in the host–guest complexation between resorcinol cyclic tetramer and organic monool compounds, the presence of an attractive interaction has been postulated.[18] However, this complexation was strongly assisted by hydrogen-bonding interactions. Direct characterization of these weak interactions is very difficult in any case.

Previously, in the complexation of *N*-pyridoxy-L-phenylalanine† with Co^{III} we suggested that the pyridoxy 2-methyl group causes an inductive CH · · · π interaction with both of pyridoxy pyridine and phenylalanyl benzene rings.[19] The *N*-pyridoxy-L-amino acid is a derivative of vitamin B_6 coenzyme, pyridoxal 5-phosphate, which plays an important role in amino acid metabolism, and the biological significance of the functional groups of the pyridoxal, *i.e.* pyridyl 1-N, 3-O and 4-azomethine in its metabolic intermediate, and 5-phosphate ester, has long been discussed by many chemists, biochemists, and biologists.[20–25] That of the pyridoxy 2-methyl group, however, is still now open to detailed investigations. In the present paper, focusing upon a possible CH · · · π interaction of this group in the pyridoxal coenzyme system, we describe a further examination on the CH · · · π interaction by use of other aliphatic or aromatic amino acids in the place of phenylalanine by means of electronic absorption (UV/VIS), circular dichroism (CD), and ^{1}H NMR spectra and crystal structure analysis. The findings obtained are interesting from the view point of molecular recognition.[19]

† Pyridoxy = 3-hydroxy-5-hydroxymethyl-2-methylpyridin-4-ylmethyl; pyridoxal = 3-hydroxy-5-hydroxymethyl-2-methylpyridine-4-carbaldehyde.

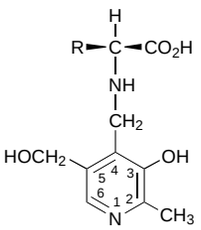

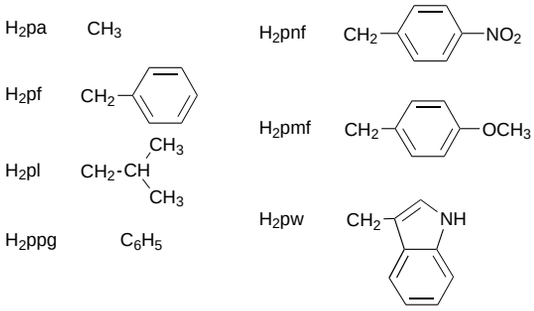

Experimental

Synthesis

***N*-Pyridoxy amino acids.** A mixture of L-amino acid (20 mmol), KOH (40 mmol), and pyridoxal hydrochloride (20 mmol) in MeOH (40 cm^3) was stirred at room temperature until it became yellow. The pyridoxylidene-L-amino acid Schiff-base solution was then treated with hydrogen gas (3 atm, *ca.* 3×10^5 Pa) for 3–4 h in the presence of PtO_2 (0.2 g). Following filtration, an appropriate amount of methanolic HCl was added to afford a quantitative yield of the *N*-pyridoxy-L-amino acid hydrochloride. These were characterized by ^{1}H NMR spectroscopy as follows.

H_2pa: δ 7.54 (s, 1 H, pyridoxal 6-H), 4.58 (s, 2 H, pyridoxal 5-CH_2), 4.18 (d, 1 H, J = 13.2, pyridoxal 4-CH_2), 4.07 (d, 1 H, J = 13.2, pyridoxal 4-CH_2), 3.45 (q, 1 H, J = 7.2, α-H of amino acid), 2.33 (s, 3 H, pyridoxal 2-CH_3), 1.40 (d, 3 H, J = 7.2 Hz, β-CH_3). H_2pf: δ 7.58 (s, 1 H, pyridoxal 6-H), 7.34 (dd, 2 H, J = 7.6 and 6.4, benzene), 7.31 (t, 1 H, J = 6.4, benzene), 7.21 (d, 2 H, J = 7.6, benzene), 4.49 (s, 2 H, pyridoxal 5-CH_2), 4.16 (d, 1 H, J = 14.0, pyridoxal 4-CH_2), 3.93 (d, 1 H, J = 14.0, pyridoxal 4-CH_2), 3.56 (dd, 1 H, J = 7.9 and 5.4, α-H of amino acid), 3.12 (dd, 1H, J = 14.1 and 5.4, β-H of amino acid), 2.95 (dd, 1 H, J = 14.1 and 7.9 Hz, β-H of amino acid) and 2.25 (s, 3 H, pyridoxal 2-CH_3). H_2pl: δ 7.49 (s, 1 H, pyridoxal 6-H), 4.59 (d, 1 H, J = 12.1, pyridoxal 5-CH_2), 4.51 (d, 1 H, J = 12.1, pyridoxal 5-CH_2), 3.92 (d, 1 H, J = 12.1, pyridoxal 4-CH_2), 3.59 (d, 1 H, J = 12.1, pyridoxal 4-CH_2), 3.22 (dd, 1 H, J = 7.3 and 7.0, α-H of amino acid), 2.31 (s, 3 H, pyridoxal 2-CH_3), 1.60–1.30 (m, 3 H, β- and γ-H of amino acid), 0.89 (d, 3 H, J = 6.4, δ-H of amino acid) and 0.84 (d, 3 H, J = 6.4 Hz, δ-H of amino acid). H_2ppg: δ 7.44 (s, 1H, pyridoxal 6-H), 7.36–7.41 (m, 5 H, benzene), 4.41 (d, 1 H, J = 12.2, pyridoxal 5-CH_2), 4.38 (d, 1 H, J = 12.2, pyridoxal 5-CH_2), 4.24 (s, 1 Hz, α-H of amino acid), 3.88 (d, 1 H, J = 12.2, pyridoxal 4-CH_2), 3.66 (d, 1 H, J = 12.2 Hz, pyridoxal 4-CH_2) and 2.31 (s, 3H, pyridoxal 2-CH_3). H_2pnf: δ 7.55 (s, 1 H, pyridoxal 6-H), 7.00 (d, 2 H, J = 7.5, benzene), 6.74 (d, 2 H, J = 7.5, benzene), 4.56 (s, 2 H, pyridoxal 5-CH_2), 4.36 (d, 1 H, J = 14.2, pyridoxal 4-CH_2), 4.18 (d, 1 H, J = 14.2, pyridoxal 4-CH_2), 3.78 (dd, 1 H, J = 8.7 and 4.4, α-H of amino acid), 3.19 (dd, 1 H, J = 15.0 and 4.4, β-H of amino acid), 2.94 (dd, 1 H, J = 15.0 and 8.7 Hz, β-H of amino acid) and 2.36 (s, 3 H, pyridoxal 2-CH_3). H_2pmf: δ 7.54 (s, 1 H, pyridoxal 6-H), 7.14 (d, 2 H, J = 8.4, benzene), 6.90 (d, 2 H, J = 8.4, benzene), 4.55 (s, 2 H, pyridoxal 5-CH_2), 4.35 (d, 1 H, J = 14.0, pyridoxal 4-CH_2), 4.16 (d, 1 H, J = 14.0, pyridoxal 4-CH_2), 3.82 (s, 3 H, methoxy), 3.78 (dd, 1 H, J = 8.8 and 4.6, α-H of amino acid), 3.23 (dd, 1 H, J = 15.0 and 4.6, β-H of amino acid), 2.97 (dd, 1 H, J = 15.0 and 8.8 Hz, β-H of amino acid) and 2.31 (s, 3 H, pyridoxal 2-CH_3). H_2pw: δ 7.65 (d, 1 H, J = 7.9, indole 4-H), 7.47 (d, 1 H, J = 8.1, indole 7-H), 7.42 (s, 1 H, pyridoxal 6-H), 4.44 (d, 1 H, J = 12.4, pyridoxal 5-CH_2), 7.22 (dd, 1 H, J = 7.9 and 7.2, indole 5-H), 7.15 (s, 1 H, indole 2-H), 7.12 (dd, 1 H, J = 8.1 and 7.2, indole 6-H), 4.16 (d, 1 H, J = 12.4, pyridoxal 5-CH_2), 3.94 (d, 1 H, J = 12.1, pyridoxal 4-CH_2), 3.57 (d, 1 H, J = 12.1, pyridoxal 4-CH_2), 3.55 (dd, 1 H, J = 7.3 and 6.4, α-H of amino acid), 3.13 (dd, 1 H, J = 14.4 and 6.4, β-H of amino acid), 3.01 (dd, 1 H, J = 14.4 and 7.3 Hz, β-H of amino acid) and 2.28 (s, 3 H, pyridoxal 2-CH_3).

Cobalt complexes. All cobalt(III) complexes were prepared as follows. To an aqueous solution (25 cm^3) of $K_3[Co(CO_3)_3]$ (1.25 mmol) was added *N*-pyridoxy-L-amino acid hydrochloride (2.5 mmol) and the mixture stirred for 12 h at room temperature. The resulting mixture was passed through a column of QAE Sephadex A-25 resin (Cl^- form, 3.6 × 25 cm), and the adsorbed compounds separated using aqueous 0.1 M NaCl. One brown band was eluted. Desalting with ethanol gave the sodium bis(*N*-pyridoxyamino acidato)cobalt(III) complex as a brown solid; 40% yield for $Na[Co(pa)_2]\cdot 5.5H_2O$ (Found: C, 40.44; H, 6.02; N, 8.74. Calc. for $C_{22}H_{28}CoN_4NaO_8\cdot 5.5H_2O$ **1**: C, 40.19; H, 5.98; N, 8.51%). Yields of the other complexes were as follows: 32% for $Na[Co(pf)_2]$ **2**, 48% for $Na[Co(pl)_2]$ **3**, 26% for $Na[Co(ppg)_2]$ **4**, 20% for $Na[Co(pnf)_2]$ **5**, 9.0% for $Na[Co(pmf)_2]$ **6** and 4.3% for $Na[Co(pw)_2]$ **7**. ^{1}H NMR spectra data (400 MHz D_2O) were as follows. $Na[Co(pa)_2]$ **1**: δ 7.79 (s, 1 H, pyridoxal 6-H), 4.87 (d, 1 H, J = 12.5, pyridoxal 5-CH_2), 4.83 (d, 1 H, J = 12.5, pyridoxal 5-CH_2), 4.59 (d, 1 H, J = 12.5, pyridoxal 4-CH_2), 4.10 (d, 1 H, J = 12.5, pyridoxal 4-CH_2), 4.37 (q, 1 H, J = 7.0, α-H of amino acid), 1.18 (s, 3 H, pyridoxal 2-CH_3) and 1.86 (d, 3 H, J = 7.0 Hz, β-CH_3). $Na[Co(pf)_2]$ **2**: δ 7.71 (s, 1 H, pyridoxal 6-H), 7.50 (d, 2 H, J = 7.3, benzene), 7.36 (dd, 2 H, J = 7.3 and 7.3, benzene), 7.28 (t, 1 H, J = 7.3, benzene), 4.77 (s, 2 H, pyridoxal 5-CH_2), 4.71 (dd, 1 H, J = 5.7 and 3.4, α-H of amino acid), 4.54 (d, 1 H, J = 12.8, pyridoxal 4-CH_2), 4.02 (d, 1 H, J = 12.8, pyridoxal 4-CH_2), 3.82 (dd, 1 H, J = 14.8 and 5.7, β-CH_2), 3.62 (dd, 1 H, J = 14.8 and 3.4 Hz, β-CH_2) and 0.84 (s, 3 H, pyridoxal 2-CH_3). $Na[Co(pl)_2]$ **3**: δ 7.87 (s, 1 H, pyridoxal 6-H), 4.93 (d, 1 H, J = 12.7, pyridoxal 5-CH_2), 4.84 (d, 1 H, J = 12.7, pyridoxal 5-CH_2), 4.67 (d, 1 H, J = 12.7, pyridoxal 4-CH_2), 4.18 (d, 1 H, J = 12.7, pyridoxal 4-CH_2), 4.35 (dd, 1 H, J = 3.2 and 2.4, α-H of amino acid), 2.40–2.05 (m, 3 H, β- and γ-H of amino acid), 1.31 (s, 3 H, pyridoxal 2-CH_3), 1.13 (d, 3 H, J = 6.4, δ-H of amino acid) and 1.05 (d, 3 H, J = 6.4 Hz, δ-H of amino acid). $Na[Co(ppg)_2]$ **4**: δ 7.72 (s, 1 H, pyridoxal 6-H), 7.69–7.62 (m, 5 H, benzene), 5.44 (s, 1 H, α-H of amino acid), 4.52 (d, 1 H, J = 12.2, pyridoxal 5-CH_2), 4.42 (d, 1 H, J = 12.2, pyridoxal 5-CH_2), 4.38 (d, 1 H, J = 12.2, pyridoxal 4-CH_2), 4.28 (d, 1 H, J = 12.2 Hz, pyridoxal 4-CH_2) and 1.17 (s, 3 H, pyridoxal 2-CH_3). $Na[Co(pnf)_2]$ **5**: δ 7.71 (s, 1 H, pyridoxal 6-H), 7.27 (d, 2 H, J = 8.1, benzene), 6.76 (d, 2 H, J = 8.1, benzene), 4.75 (s, 2 H, pyridoxal 5-CH_2), 4.64 (dd, 1 H, J = 5.5 and 2.9, α-H of amino acid), 4.53 (d, 1 H, J = 12.8, pyridoxal 4-CH_2), 4.02 (d, 1 H, J = 12.8, pyridoxal 4-CH_2), 3.71 (dd, 1 H, J = 15.0 and 5.5, β-H of amino acid), 3.51 (dd, 1 H, J = 15.0 and 2.9 Hz, β-H of amino acid) and 0.87 (s, 3 H, pyridoxal 2-CH_3). $Na[Co(pmf)_2]$ **6**: δ 7.70 (s, 1 H, pyridoxal 6-H), 7.42 (d, 2 H, J = 8.6, benzene), 6.94 (d, 2 H, J = 8.6, benzene), 4.76 (s, 2 H, pyridoxal 5-CH_2), 4.67 (dd, 1 H, J = 5.6 and 3.0, α-H of amino acid), 4.52 (d, 1 H, J = 12.8, pyridoxal 4-CH_2), 4.02 (d, 1 H, J = 12.8, pyridoxal 4-CH_2), 3.88 (s, 3 H, methoxy), 3.78 (dd, 1 H, J = 15.0 and 5.6, β-H of amino acid), 3.58 (dd, 1 H, J = 15.0 and 3.0 Hz, β-H of amino acid) and 0.83 (s, 3 H, pyridoxal 2-CH_3). $Na[Co(pw)_2]$ **7**: δ 7.84 (d, 1 H, J = 7.9, indole 4-H), 7.63 (s, 1 H, pyridoxal 6-H), 7.42 (s, 1 H, indole 2-H), 7.41 (d, 1 H, J = 8.1, indole 7-H), 7.19 (dd, 1 H, J = 7.9 and 7.0, indole 5-H), 7.13 (dd, 1 H, J = 8.1 and 7.0, indole 6-H), 4.55 (d, 1 H, J = 12.8,

pyridoxal 5-CH_2), 4.51 (d, 1 H, J = 12.8, pyridoxal 5-CH_2), 4.47 (d, 1 H, J = 12.1, pyridoxal 4-CH_2), 4.00 (d, 1 H, J = 12.1 Hz, pyridoxal 4-CH_2), 0.73 (s, 3 H, pyridoxal 2-CH_3); α- and β-protons of amino acid moiety were not identified.

Protonation

The complex Na[Co(pa)$_2$] **1** was protonated by addition of HCl, the progress of which was monitored by UV/VIS, CD and ^{1}H NMR spectra. The proton number and protonation constant were estimated by use of a CD spectrophotometer. The pH values were measured with an Orion Research pH-meter, model EA-920. Hydrogen-ion concentration, [H^+], was calculated from $a_{H^+}/\gamma_{\pm}$, using $\gamma_{\pm} = 0.83$.[26]

On standing for several days an aqueous solution of complex **2** gave dark brown crystals (**2′**) (Found: C, 56.41; H, 7.97; N, 5.53. Calc. for $C_{34}H_{37}CoN_4O_8 \cdot 2H_2O$: C, 56.35; H, 7.73; N, 5.56%).

Measurements

Electronic absorption spectra were recorded on a JASCO UVIDEC-660 spectrophotometer, and circular dichroism spectra on a JASCO J-500C spectropolarimeter (0.01–1 mM solutions in D_2O, room temperature). Proton NMR spectra were recorded on a JEOL JNM-GX 400 MHz spectrometer in $(CD_3)_2SO$ and CD_3OD ($SiMe_4$ as reference) and in D_2O [sodium 4,4-dimethyl-4-silapentanesulfonate (dss) as reference].

Crystallography

Single crystals of Na[Co(pa)]·5.5H_2O **1** and Na[Co(pf)]·6H_2O **2** suitable for X-ray analyses were recovered from eluates following chromatography and standing for several days. Those of **2′** were obtained from a solution of **2** prepared by addition of 1 equivalent HCl. Crystal data and experimental details are summarized in Table 3. Diffraction data were collected at 293 K with an Enraf-Nonius CAD4-EXPRESS four-circle automated diffractometer. The crystals were sealed in a glass capillary tube to avoid loss of water. Reflection intensities were monitored by three standard reflections every 2 h, and the decay was within 2% in each case. Reflection data were corrected for Lorentz and polarization effects. An empirical absorption correction, based on ψ scans, was applied.

The structures were solved by the heavy-atom method and refined anisotropically for non-hydrogen atoms by full-matrix least-squares calculations. Refinements were continued until all shifts were smaller than one-third of the standard deviations of the parameters involved. Atomic scattering factors and anomalous dispersion terms were taken from ref. 27. The positions of hydrogen atoms except those of the pyridinium moieties of complex **2′** and water molecules were obtained from the Fourier-difference maps, and their parameters were isotropically refined. The R and R' values were 0.0541 and 0.0631 for **1**, 0.0638 and 0.0765 for **2**, and 0.0406 and 0.0449 for **2′** respectively. The weighting scheme $w^{-1} = \sigma^2(F_o) + (0.015F_o)^2$ was employed for all crystals. The final Fourier-difference maps did not show any significant features. The calculations were performed on a Micro VAX-3100 computer using the program system SDP-MOLEN.[28] Selected bond lengths and angles are listed in Table 4.

CCDC reference number 186/657.

Results

Syntheses

The *N*-pyridoxy-L-amino acids H_2L were synthesized from the corresponding L-amino acid and pyridoxal by the reductive alkylation method. The reaction of H_2L with $K_3[Co(CO_3)_3]$ in a 2:1 molar ratio gave the complex anions $[CoL_2]^-$. As shown below, they are optically active and their crystals are asymmetric. This indicates that an isomer was formed selectively under the preparation conditions, although many kinds of isomers, such as *trans*(N) or *cis*(N) for the arrangement of donor atoms, meridional or facial for the configuration of chelate rings, Δ or Λ for the helicity of two unsymmetrical tridentate ligands, *R* or *S* for the configuration of asymmetric nitrogen atoms of the amino acid moiety, *etc*., are possible for these complexes (Scheme 1). In the course of complexation of the *N*-pyridoxyamino acid with cobalt ion, some regulation may occur through an intramolecular ligand–ligand interaction.

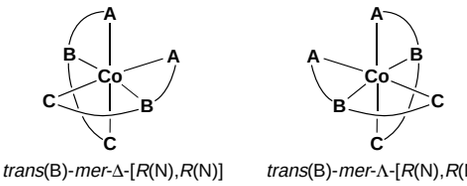

Scheme 1 A, B and C denote the co-ordinated atoms of the *N*-pyridoxy-L-amino acid, *i.e.* carboxylate oxygen, amino nitrogen and phenol oxygen

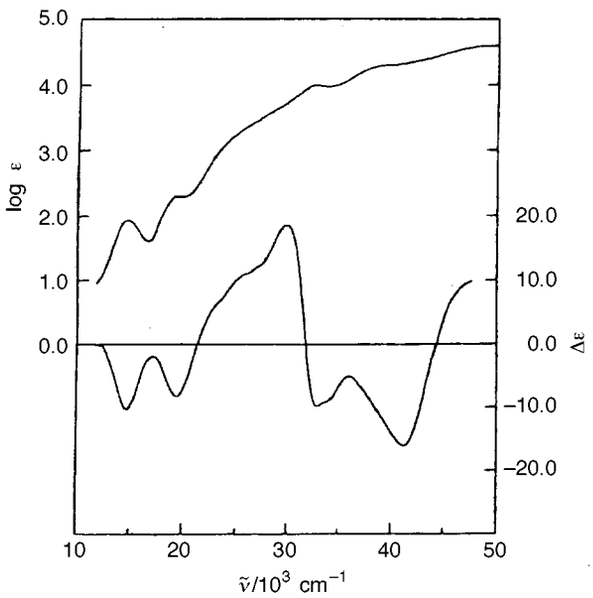

Fig. 1 Electronic absorption (upper) and circular dichroism (lower) spectra of the complex Na[Co(pa)$_2$] **1**

UV/VIS and CD spectra

The electronic absorption spectrum of the Na[Co(pa)$_2$] **1** complex as a typical example is given in Fig. 1 together with the CD spectrum. Well separated first absorption bands were observed near 15 000 and 20 000 cm^{-1}, which is a typical spectral pattern for a complex of *trans*(X)-[CoX_2Y_4] type.[29] Similar spectra were observed for all other complexes as summarized in Table 1. Since the spectral patterns of the well separated first absorption bands resemble well those of a bis(pyridoxylidene-L-phenylalaninato)cobaltate complex anion with a meridional *trans*(N) configuration, these cobalt(III) complexes are also expected to take the same configuration.[30]

Corresponding to the well separated first absorption bands, two negative CD bands were observed in the same spectral region. The spectral patterns for complexes **2**–**7** are essentially the same as that for **1**. The electronic absorption and CD spectra for **1**–**7** were the same both in isolated crystals and in their mother-liquors, indicating that all these complexes have the same absolute configuration in both the solid and solution states and that the co-ordination geometries around the central metal ion are not affected by the difference in amino acid side chains.

Table 1 Electronic absorption and CD spectral data for the $Na[CoL_2]$ complexes*

Complex	Absorption (log ε)	CD (Δε)
1 $Na[Co(pa)_2]$	14.6 (1.93)	14.5 (−10.1)
	19.3 (2.32)	19.4 (−8.2)
	24.5 (3.28, sh)	24.1 (+6.0)
		25.4 (+11.0)
		30.0 (+18.9)
2 $Na[Co(pf)_2]$	14.9 (1.78)	14.8 (−8.3)
	19.8 (2.36, sh)	19.3 (−6.4)
	24.0 (3.09, sh)	26.9 (+17.3, sh)
		30.0 (+19.2)
3 $Na[Co(pl)_2]$	14.9 (1.78)	14.9 (−6.5)
	19.3 (2.16)	19.4 (−3.4)
	24.7 (2.97, sh)	23.8 (+2.1, sh)
		22.9 (+7.7)
		29.7 (+12.5)
4 $Na[Co(ppg)_2]$	14.7 (1.88)	14.8 (−7.9)
	19.3 (2.26, sh)	19.4 (−5.6)
	23.7 (3.28, sh)	22.0 (+4.1, sh)
		24.6 (+6.8, sh)
		28.3 (+8.8)
		30.0 (+9.0)
5 $Na[Co(pnf)_2]$	14.9 (1.78)	14.8 (−6.9)
	19.7 (2.12, sh)	19.7 (−5.9)
	24.0 (3.06, sh)	23.7 (+5.1, sh)
		27.0 (+6.9, sh)
		30.0 (+9.0)
6 $Na[Co(pmf)_2]$	14.9 (1.78)	14.8 (−7.1)
	19.7 (2.10, sh)	19.7 (−6.0)
	24.0 (3.03, sh)	23.7 (+5.1, sh)
		27.0 (+6.9, sh)
		30.0 (+8.8)
7 $Na[Co(pw)_2]$	14.6 (1.69)	14.7 (−5.7)
	19.3 (2.00)	19.5 (−3.9)
	24.7 (2.93, sh)	23.2 (+3.4, sh)
		26.8 (+7.7, sh)
		29.7 (+7.8)

* Wavenumbers are given in 10^3 cm^{-1}; sh = shoulder.

Table 2 Proton NMR chemical shifts (δ) of the 2-methyl groups for *N*-pyridoxy-L-amino acid ligands and their cobalt(III) binary complexes in D_2O[a]

Amino acid	Free	Complexed
H_2pa	2.33	1.18 (+1.15)[b]
H_2pf	2.25	0.84 (+1.41)[b]
H_2pl	2.31	1.31 (+1.00)[b]
H_2ppg	2.31	1.17 (+1.14)[b]
H_2pnf	2.36	0.87 (+1.49)[b]
H_2pmf	2.31	0.83 (+1.48)[b]
H_2pw	2.28	0.73 (+1.55)[b]

[a] Chemical shifts from dss. [b] The difference between the 2-methyl protons for *N*-pyridoxy-L-amino acid and its cobalt(III) binary complex; + denotes an upfield shift.

^{1}H NMR spectra

In general, the ^{1}H NMR spectra of ligands show downfield shifts upon complex formation with a diamagnetic metal ion. Those of the pyridoxyamino acids prepared here also showed 0.1–1.2 ppm downfield shifts upon complex formation with Co^{III}; those of the α-hydrogen of the amino acid moieties were 1.0–1.2 ppm downfield. However, only the 2-methyl groups showed significant upfield shifts (Table 2). They were observed at concentrations less than ≈0.1 mM, which can be explained by a ring-current effect due to an intramolecular proximity between the 2-methyl group and the pyridoxal ring. This undoubtedly indicates that a CH···π interaction is present between the 2-methyl group and the pyridoxal ring in these complexes. The upfield shifts of the 2-methyl protons were larger for bis(*N*-pyridoxy-L-aromatic amino acidato)cobalt(III) complexes, such as those of pf, pnf, pmf and pw (1.41–1.55 ppm) than those of bis(*N*-pyridoxy-L-aliphatic amino acidato)-cobalt(III) complexes, such as those of pa and pl (1.00–1.15 ppm). The complex with *N*-pyridoxy-L-tryptophan having the larger aromatic side chain, $Na[Co(pw)_2]$, demonstrated the largest upfield shifts. These are explained in terms of an additional ring-current effect caused by an approach of the aromatic ring of amino acid to the 2-methyl group. The relatively small upfield shift of $[Co(ppg)_2]^-$ can be understood from the fact that the phenyl ring of ppg cannot approach the 2-methyl group, as is obvious from the Corey–Pauling–Koltun (CPK) model.

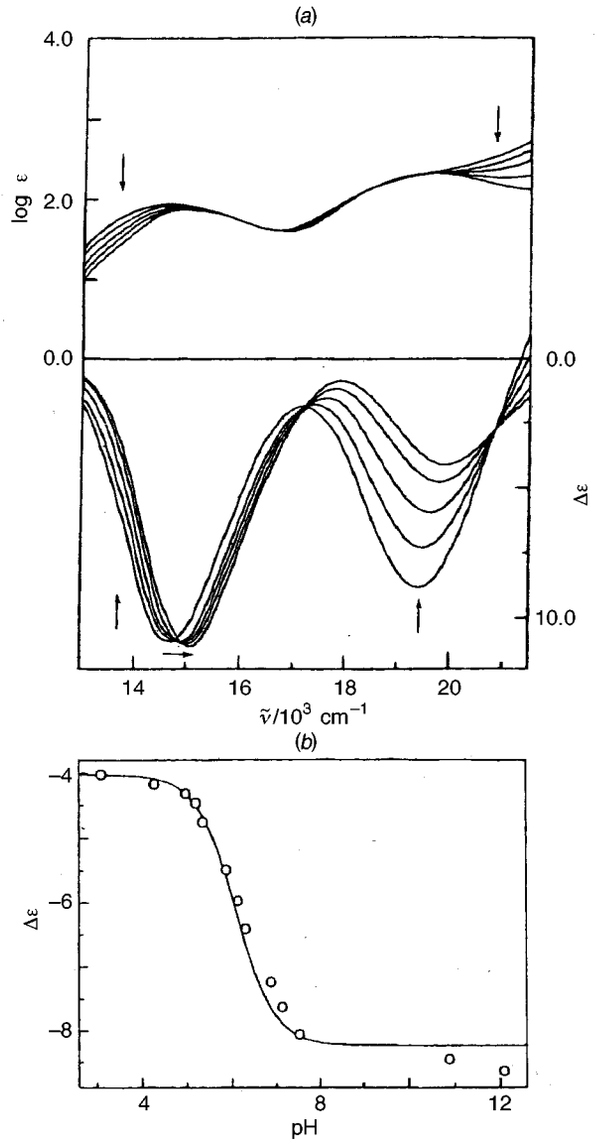

Fig. 2 (*a*) Changes in electronic absorption (upper) and circular dichroism (lower) spectra for the complex $Na[Co(pa)_2]$ **1** on protonation. (*b*) Plot of Δε *vs.* pH for the CD peak at 19 600 cm^{-1}. The curve is a theoretical one drawn by using the ideal values

Previously, the ^{1}H NMR upfield shift observed for the 2-methyl protons of bis(pyridoxylideneamino acidato)aluminium(III) complexes was described in terms of the shielding effect due to the adjacent azomethine group.[31,32] Our results, however, suggest that the upfield shift is caused by the ring current of the adjacent pyridoxy pyridine ring.

Protonation of the $[Co(pa)_2]^-$ complex in solution

The successive addition of HCl to an aqueous solution of complex **1** gave rise to a pH-dependent spectral change. The two characteristic electronic absorption and CD peaks in the region of 14 600 and 19 400 cm^{-1} demonstrated shifts to higher energy with an increase in the hydrogen-ion concentration $[H^+]$, as shown in Fig. 2(*a*), in which the CD peaks shifted with isosbes-

tic points at 16 800 and 21 000 cm^{-1}. Furthermore, the strength of the negative CD peak near 20 000 cm^{-1} decreased with increasing hydrogen-ion concentration, although such a change was not observed in the electronic absorption spectra. The higher-energy shift in the first two absorption bands and the decrease in the strength of the negative CD peak may suggest a change in the co-ordination structure around the metal ion. The protonation equilibrium of the complex **1** can be expressed by equation (1) where K_n represents the equilibrium constant

$$[Co(pf)_2]^- + nH^+ \overset{K_n}{\rightleftharpoons} [CoH_n(pf)_2]^{(n-1)+} \quad (1)$$

$$K_n = [CoH_n(pf)_2{}^{(n-1)+}]/[H^+]^n[Co(pf)_2{}^-] \quad (2)$$

and $[Co(pf)_2{}^-]$ and $[CoH_n(pf)_2{}^{(n-1)+}]$ denote the concentrations of non-protonated, $[Co(pf)_2]^-$, and protonated cobalt(III) complexes, $[CoH_n(pf)_2]^{(n-1)+}$, respectively. According to the literature,[33] equation (3) can be derived where A_{max}, A and A_{min}

$$n\cdot\log[H^+] = \log[(A - A_{min})/(A_{max} - A)] - \log K_n \quad (3)$$

represent the strength ($\Delta\varepsilon$) of the negative CD peak for $[Co(pf)_2]^-$, that for the coexisting metal complex at $[H^+]$ and that for the protonated metal complex, respectively. A plot of $\Delta\varepsilon$ for the peak at 19 600 cm^{-1} against pH is shown in Fig. 2(*b*), which gives $A_{max} = -4.03$, $A = -6.15$, $A_{min} = -8.24$ and log $K_n = 6.1$. The substitution of these values in equation (3) gave $n = 1$, and the addition of two H^+ ions does not satisfy the above theoretical equation (3). This indicates that one H^+ is added to the complex. From a comparison of the protonation constant with those reported previously for trivalent binary metal complexes of pyridoxyethane-1,2-diamine ($M = In^{III}$, Ga^{III} or Fe^{III}),[34] the protonation is considered to have occurred at pyridine nitrogen.

The ^1H NMR spectrum also showed a very interesting feature. The 2-methyl- and 6-protons of complex **1** exhibited 0.47 and 0.21 ppm downfield shifts, respectively, on protonation, although the other protons did not show any significant shifts. Furthermore, the shift of the 2-methyl protons, which are hardly affected by co-ordination, was larger than that of the 6-proton. These facts allow us to suggest that the shift of the 6-proton is caused by the protonation of the pyridine nitrogen and that the larger shift for the 2-methyl protons is due to the decrease in the intramolecular interaction between the aromatic ring and 2-methyl group. Interestingly, the downfield shift of the 2-methyl protons in complex **2**, 0.81 ppm, was much larger than that for the free pyridoxyamino acid, but the chemical shift of the 2-methyl protons for the protonated complex **2′** was almost the same as that for the protonated complex **1**. This finding may indicate that the phenyl ring of the phenylalanyl group in complex **2** also interacts with the 2-methyl group.

Crystal structures of complexes 1, 2 and 2′

As is obvious from the selected bond lengths and angles for complexes **1**, **2** and **2′** (Table 3), the co-ordinate bond parameters around the cobalt atoms are within the normal values. All these crystal structures [Figs. 3, 4(*a*) and 5, respectively] reveal that each Co^{III} is six-co-ordinated with two 3-hydroxy oxygen, two amino nitrogen, and two carboxyl oxygen atoms of two tridentate pyridoxy-L-amino acid ligands in meridional *trans*-(N) configuration, as was postulated from the spectroscopic results in the solution state. All the structures are comprised of only one diastereoisomer; the configurations around the central metal atom and around the amino nitrogen atom are Λ and *R*, respectively, *i.e.* *trans*(N)-*mer*-Λ-[*R*(*N*), *R*(*N*)]-$[CoL_2]^-$.

As predicted from the ^1H NMR upfield shift of the 2-methyl groups, the crystal structures of the complexes **1** and **2** also demonstrated an anomalous intramolecular assembly between the 2-methyl group and adjacent pyridoxy pyridine ring. The

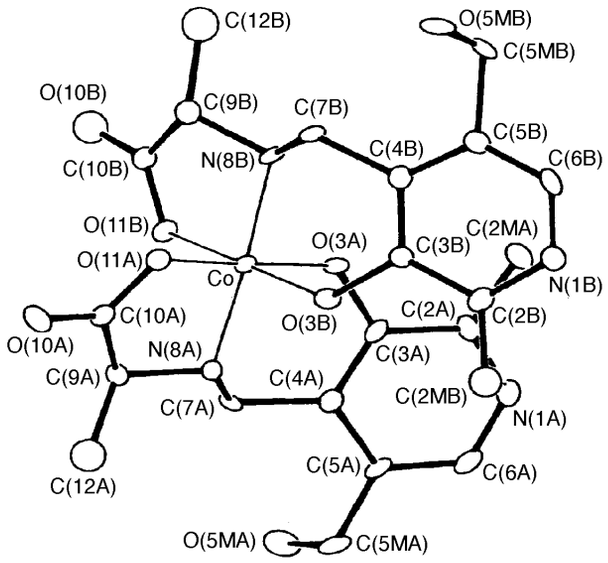

Fig. 3 An ORTEP[35] drawing of the complex anion $[Co(pa)_2]^-$ **1** showing the atom labelling scheme. Ellipsoids enclose 50% probability; H atoms are omitted for clarity

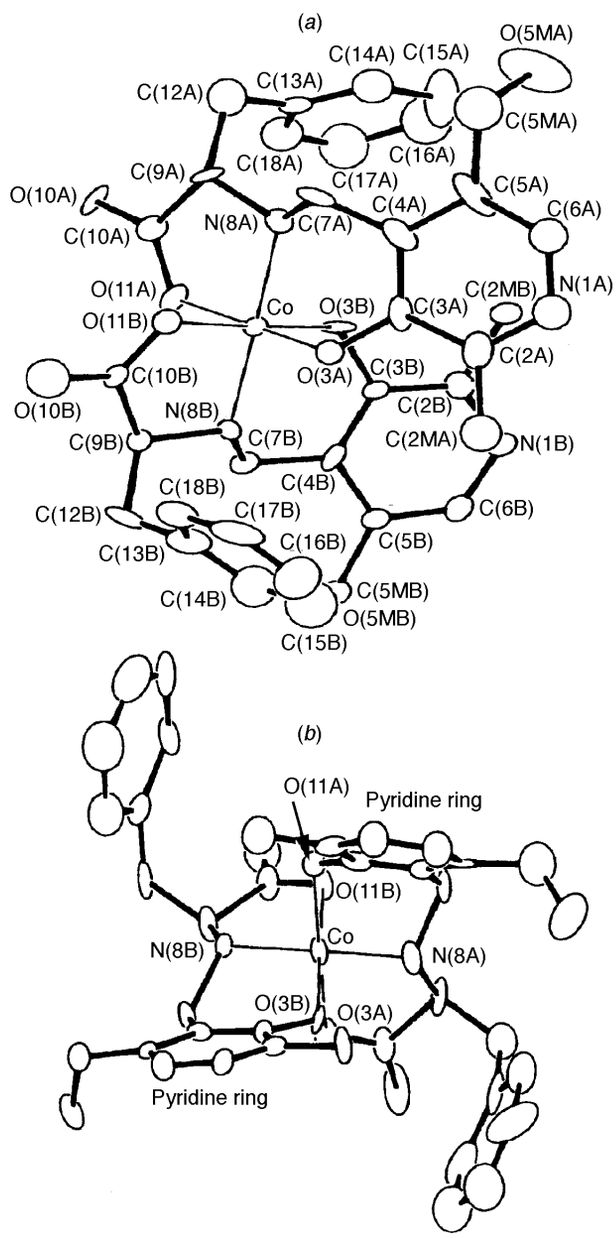

Fig. 4 (*a*) An ORTEP drawing of the complex anion $[Co(pf)_2]^-$ **2** showing the atom labelling scheme. Details as in Fig. 3. (*b*) Side view

Table 3 Crystal data and experimental details * for $Na[Co(pa)_2]\cdot 7H_2O$ **1**, $Na[Co(pf)_2]\cdot 6H_2O$ **2** and $[CoH(pf)_2]\cdot 2H_2O$ **2′**

	1	**2**	**2′**
Formula	$C_{22}H_{28}CoN_4NaO_8\cdot 7H_2O$	$C_{34}H_{36}CoN_4NaO_8\cdot 6H_2O$	$C_{34}H_{37}CoN_4O_8\cdot 2H_2O$
M	684.5	818.7	724.6
Crystal size/mm	0.6 × 0.3 × 0.2	0.5 × 0.3 × 0.2	0.3 × 0.3 × 0.3
Crystal system	Monoclinic	Orthorhombic	Monoclinic
Space group	$P2_1$	$P2_12_12_1$	$C2$
a/Å	9.5478(3)	8.719(1)	15.272(1)
b/Å	15.912(2)	20.151(2)	13.852(1)
c/Å	10.585(2)	21.993(2)	9.200(1)
β/°	90.770(9)	—	116.929(4)
U/Å^3	1607.9(3)	3864.2(6)	1735.4(2)
Z	2	4	2
$2\theta_{max}$/°	52.64	52.64	52.64
D_c/g cm^{-3}	1.41	1.41	1.39
μ/cm^{-1}	6.11	5.20	5.51
Transmission coefficient range	0.89–1.11	0.85–1.09	0.93–1.01
No. reflections observed	3555	4381	1837
No. reflections used [$I_o > 3\sigma(I_o)$]	3546	2920	1429
R	0.0541	0.0638	0.0406
R'	0.0631	0.0765	0.0449

* In common: dark brown; ω–2θ scans; λ(Mo-Kα) 0.710 73 Å.

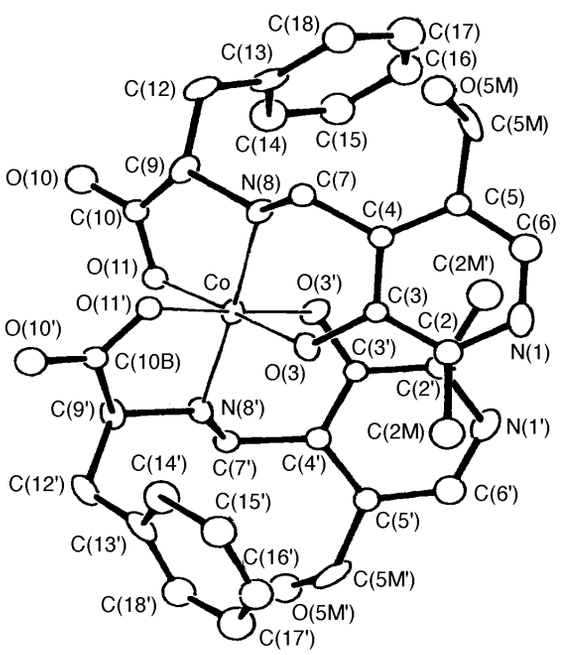

Fig. 5 An ORTEP drawing of the complex $[CoH(pf)_2]$ **2′** showing the atom labelling scheme. Details as in Fig. 3

separations between the 2-methyl carbon and another pyridine ring plane were 3.67 and 3.67 Å for complex **1** and 3.52 and 3.62 Å for **2**, respectively, the former of which are comparable to the sum (3.7 Å) of the van der Waals radii of the methyl group (2.0 Å) and aromatic carbon (1.7 Å)[36] and the latter of which are slightly shorter in comparison. Simultaneously, the two pyridine rings also showed intramolecular stacking with mean separations 3.29 and 3.59 Å and with tilting angles of 43.4 and 24.5°, respectively, which may also contribute to the intramolecular C–H · · · π interaction. Such an abnormal assembly must cause great strain around the metal ion, as is evident from CPK model considerations, and there is great distortion around the metal atom [Fig. 4(*b*)].

Furthermore, in the crystal structure of complex **2** the phenyl ring plane also approached the 2-methyl group, although at distances of 3.92 and 4.26 Å. Such an additional interaction is supported by the fact that the ^{1}H NMR upfield shift of the 2-methyl protons in **2** in D_2O is larger by 0.34 ppm than that in **1** having no phenyl group. A similar upfield shift has also been observed in CD_3OD or $(CD_3)_2SO$ solutions. These facts indicate that the attractive approach of the phenyl ring to the 2-methyl group occurs in both solid and solution states.

As described above, the UV/VIS, CD and ^{1}H NMR spectral changes upon protonation of complex **2** suggested some structural changes in the solution phase. Fortunately, we obtained

Table 4 Selected bond lengths (Å) and angles (°) for complexes **1**, **2** and **2′**

Complex **1**			
Co–O(3A)	1.890(3)	Co–O(3B)	1.884(3)
Co–O(11A)	1.884(3)	Co–O(11B)	1.899(3)
Co–N(8A)	1.930(4)	Co–N(8B)	1.927(4)
O(3A)–Co–O(3B)	91.5(1)	O(3A)–Co–O(11A)	178.4(1)
O(3A)–Co–O(11B)	89.3(1)	O(3A)–Co–N(8A)	96.1(1)
O(3A)–Co–N(8B)	86.3(1)	O(3B)–Co–O(11A)	89.6(1)
O(3B)–Co–O(11B)	178.7(1)	O(3B)–Co–N(8A)	86.0(1)
O(3B)–Co–N(8B)	96.5(1)	O(11A)–Co–O(11B)	89.6(1)
O(11A)–Co–N(8A)	85.1(1)	O(11A)–Co–N(8B)	92.5(1)
O(11B)–Co–N(8A)	92.8(1)	O(11B)–Co–N(8B)	84.6(1)
N(8A)–Co–N(8B)	176.5(2)		
Complex **2**			
Co–O(3A)	1.874(5)	Co–O(3B)	1.868(5)
Co–O(11A)	1.903(5)	Co–O(11B)	1.929(5)
Co–N(8A)	1.911(7)	Co–N(8B)	1.911(6)
O(3A)–Co–O(3B)	93.9(2)	O(3A)–Co–O(11A)	175.9(2)
O(3A)–Co–O(11B)	88.9(2)	O(3A)–Co–N(8A)	93.6(3)
O(3A)–Co–N(8B)	87.7(2)	O(3B)–Co–O(11A)	90.1(2)
O(3B)–Co–O(11B)	176.8(2)	O(3B)–Co–N(8A)	85.1(2)
O(3B)–Co–N(8B)	95.7(2)	O(11A)–Co–O(11B)	87.1(2)
O(11A)–Co–N(8A)	85.8(3)	O(11A)–Co–N(8B)	92.9(2)
O(11B)–Co–N(8A)	93.3(2)	O(11B)–Co–N(8B)	85.9(2)
N(8A)–Co–N(8B)	178.4(3)		
Complex **2′** *			
Co–O(3)	1.890(3)	Co–O(11)	1.903(3)
Co–N(8)	1.935(2)		
O(3)–Co–O(3′)	91.9(1)	O(11)–Co–N(8)	85.2(2)
O(3)–Co–O(11′)	89.8(1)	O(11′)–Co–N(8)	93.1(2)
O(3)–Co–N(8′)	85.4(2)	O(11)–Co–O(11′)	88.5(1)
O(3′)–Co–O(11′)	177.9(1)	N(8)–Co–N(8′)	177.7(2)
O(3′)–Co–N(8′)	96.2(2)		

* Atoms corresponding to the other half of the dimer are denoted by primes.

Table 5 Proton NMR chemical shifts (ppm) of complexes **1** and **2** in D_2O on protonation [a]

	Na[Co(pa)$_2$] **1**		Na[Co(pf)$_2$] **2**	
	2-CH_3	6-H	2-CH_3	6-H
Complex (pH ≈ 7)	1.18(+1.15) [b]	7.79(−0.25)	0.84(+1.41)	7.79(−0.21)
Protonated complex (pH ≈ 2)	1.65(+0.68)	8.00(−0.46)	1.65(+0.60)	7.89(−0.31)
Free pyridoxyamino acid	2.33	7.54	2.25	7.58

[a] Chemical shifts from dss. [b] The values in parentheses denote the differences between chemical shifts of the complexes and free pyridoxyamino acids, and + and − denote up- and down-field shifts.

Table 6 Upfield ^{1}H NMR chemical shifts (ppm) estimated according to the Johnson and Bovey [37] equation

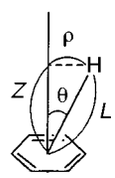

	Ring-current effect by pyridine ring *			Ring-current effect by benzene ring *		
	H(2MA)	H(2MB)	H(2MC)	H(2MA)	H(2MB)	H(2MC)
L/Å	2.998	3.681	4.481	4.111	5.288	4.505
θ/°	7.35	17.49	3.97	28.39	24.94	9.85
Z/Å	2.97	3.51	4.47	3.96	4.80	4.44
ρ/Å	0.84	1.11	0.31	1.96	2.23	0.77
Calculated upfield shift (ppm)	1.60	0.93	0.59	0.43	0.26	0.56
Average of upfield shifts (ppm)		1.04			0.42	

* Co-ordinates of hydrogen atoms H(2MA), H(2MB) and H(2MC) established for complex **2** were employed to estimate the ring-current effect by pyridine and benzene rings.

single crystals of monoprotonated complex **2′**. The structure has almost the same configuration as those of complexes **1** and **2**. Subtle but clear differences, however, were detected in the bond lengths around the metal ions; the Co–O and Co–N bonds for complex **2′** are respectively shorter and longer on average in comparison with those for **2** as can be seen from Table 4. The proton in **2′** seems to be located on the pyridoxal nitrogen atoms, which is supported by the fact that the solvated water molecule O(1W) is associated with the two nitrogen atoms, N(1)···O(1W) 2.66 Å. The distance between the pyridoxal mean plane and the adjacent 2-methyl carbon, 3.56 Å, was almost the same as those for complex **2**, although the two pyridoxal rings approached each other with a distance of 3.32 Å and a tilting angle of 17.3°. As expected from the difference in the ^{1}H NMR chemical shifts of the 2-methyl protons for complexes **2** and **2′** (Table 5), the phenyl ring of **2′** was removed from the 2-methyl group with a distance of 4.45 Å in comparison with that in **2** (3.92 and 4.26 Å), which may be explained by considering that there exists a repulsive intramolecular, interligand interaction between the phenyl and the pyridoxal groups.

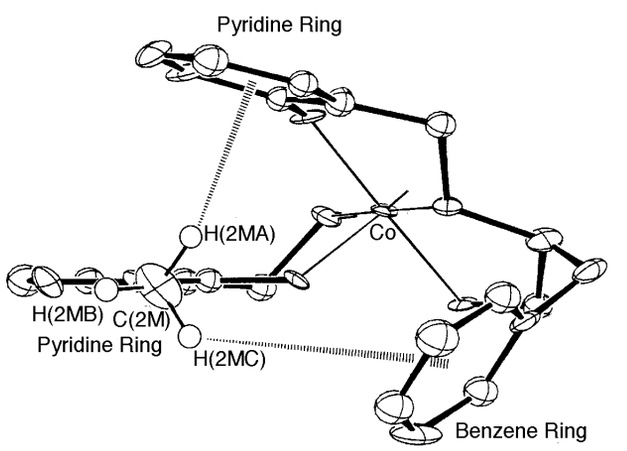

Fig. 6 View of the [CoH(pf)$_2$] complex **2′** showing the manner of CH···π interactions, with the atomic labelling scheme. Ellipsoids enclose 50% probability; H atoms except for those of the 2-methyl group are omitted for clarity

Discussion

CH···π Interaction in solution and solid states

The ^{1}H NMR spectra of the pyridoxy 2-methyl groups in these complexes all exhibited upfield shifts in comparison with those in the free pyridoxyamino acids; the magnitude of the shifts was in the order, pw > pnf, pmf > pf > pa, ppg > pl, as is obvious from Table 2. These upfield shifts can be explained by the ring-current effect due to the intramolecular proximity between the 2-methyl group and the pyridoxal ring, as is suggested from the crystal structures of the Na[Co(pa)$_2$] and Na[Co(pf)$_2$] complexes. Such large shifts are specific to the bis(*N*-pyridoxy-L-amino acidato)cobalt(III) complexes with aromatic side chains, such as those of pf, pnf, pmf and pw. In view of the crystal structure of the Na[Co(pf)$_2$] complex, which shows an intramolecular approach of the phenyl ring of the amino acid side chain to the pyridoxy 2-methyl group, it may be suggested that the larger ^{1}H NMR upfield shifts are due to the ring-current effect by the aromatic side chains in addition to that by the pyridoxal pyridine ring: the order of these upfield shifts corresponds to that of the sizes of the aromatic rings. The larger shift in the [Co(pw)$_2$]$^-$ complex anion strongly supports this consideration.

As was previously reported, we succeeded in accurate determination of the crystal structure of the complex Na[Co(pf)$_2$] **2**.[19] It revealed that two of the three C–H bond vectors of the 2-methyl group were directed in the planes of the pyridoxy pyridine and phenylalanyl benzene rings of the neighbouring ligand (Fig. 6). The hydrogen atoms of the 2-methyl

groups in complexes **1** and **2** obtained from the Fourier-difference maps were also oriented in the same manner as those in **2′**. The presence of an interaction in the latter is also supported by the fact that the ^{1}H NMR upfield shift of the 2-methyl protons in **2** is larger by 0.34 ppm than that in **1**, although the separations between the 2-methyl carbon and phenyl ring (3.92 and 4.26 Å) are long. It is concluded from these results that such an anomalous arrangement of aromatic rings with respect to the 2-methyl group is enforced by the CH · · · π interaction.

In order to explain the magnitude of the upfield shifts in ^{1}H NMR spectra stated above and the anomalous arrangement of aromatic rings in the crystal structure, the shift values due to the ring-current effect were estimated by using the coordinates of the Na[Co(pf)$_2$] crystal established here according to the equation of Johnson and Bovey.[37] Table 6 shows that the estimated ring-current shift values by pyridine and benzene rings are 1.04 and 0.42 ppm, respectively. Interestingly, the latter value is unexpectedly large and the sum of the calculated upfield shifts (1.46 ppm) is in striking agreement with the experimental value (1.41 ppm), which may indicate that the conformation demonstrated in the crystals is maintained also in solution.

The protonation of the pyridoxy pyridine nitrogen resulted in a reduction in the strength of negative CD peak near 20 000 cm^{-1} and a downfield shift in the ^{1}H NMR peak of the 2-methyl group (0.81 ppm). The former may be due to the vicinal effect [38] and suggests a significant conformational change in the primnary co-ordination sphere around the central metal ion. The latter may be explained by the decrease in the CH · · · π interaction between the 2-methyl protons and the aromatic rings. These spectral features are related to the asymmetric and aromatic amino acid side chain, indicating that the aromatic rings are distant from the 2-methyl group. As was expected, the phenyl ring was removed from the 2-methyl group to a separation of 4.45 Å. The long separation in the protonated complex **2′** can be attributed to the closer contact between the two pyridine rings in comparison with that in the unprotonated complex **2**. Hence, it is concluded that protonation of pyridine nitrogen reduces the electron density on the aromatic rings and therefore weakens the interligand CH · · · π interaction.

Conclusion

Although weak bondings such as the CH · · · π interaction are affected by the solvent, they are still present in aqueous solutions, as is seen from the above-mentioned spectral findings. The *N*-pyridoxy-L-amino acids employed here are derivatives of vitamin B$_6$ coenzyme, pyridoxal-5-phosphate, which plays an important role in amino acid metabolism in biological systems, and the significance of the functional groups of the pyridoxal molecule has long been discussed by many chemists, biochemists and biologists.[20–25] However, that of the 2-methyl group is open to discussion even at present, in spite of the experimental result that the absence of the 2-methyl group from the pyridoxal coenzyme decreases vitamin B$_6$ activity.[24] The recent crystal structure analysis of aspartate aminotransferase bound to the cofactor pyridoxal 5-phosphate has demonstrated that the two aromatic rings of tyrosine and tryptophan are close to the 2-methyl group in the enzyme. The CH · · · π interactions between the 2-methyl group and aromatic rings, described in this paper, may therefore suggest that the 2-methyl group acts as the recognition group of the active site in the enzyme through the CH · · · π interaction with the aromatic rings.

Acknowledgements

Thanks are due to the Instrument Center, the Institute for Molecular Science, for assistance in obtaining the 400 MHz ^{1}H NMR spectra. This work was supported by a Grant-in-Aid for Specially Promoted Research from the Ministry of Education, Science and Culture, Japan.

References

1 B. Alberts, D. Bray, J. Lewis, M. Raff, K. Roberts and J. D. Watson, *Molecular Biology of the Cell*, Garland Publishing, New York, 3rd edn., 1994, p. 89.
2 E. Frieden, *J. Chem. Educ*., 1975, **52**, 754.
3 W. P. Jencks, *Adv. Enzymol. Relat. Areas Mol. Biol*., 1975, **43**, 219.
4 S. K. Burley, P. R. David, A. Taylor and W. N. Lipscomb, *Proc. Natl. Acad. Sci. USA*, 1990, **87**, 6878.
5 S. K. Burley, P. R. David, R. M. Sweet, A. Taylor and W. N. Lipscomb, *J. Mol. Biol*., 1992, **224**, 113.
6 H. Kim, S. K. Burley and W. N. Lipscomb, *J. Mol. Biol*., 1993, **230**, 722.
7 S. K. Burley, P. R. David, R. M. Sweet and W. N. Lipscomb, *Proc. Natl. Acad. Sci. USA*, 1991, **88**, 6919.
8 T. Mizutani, T. Ema, T. Tomita, Y.Kuroda and H. Ogoshi, *J. Am. Chem. Soc*., 1994, **116**, 4240.
9 H. Masuda, A. Odani, T. Yamazaki, T. Yajima and O. Yamauchi, *Inorg. Chem*., 1993, **32**, 1111.
10 K. Jitsukawa, T. Morioka, H. Masuda, H. Ogoshi and H. Einaga, *Inorg. Chim. Acta*, 1994, **216**, 249.
11 O. Yamauchi, A. Odani, H. Masuda and H. Sigel, *Metal Ions in Biological Systems*, eds. A. Sigel and H. Sigel, Marcel Dekker, New York, 1996, vol. 32, p. 207.
12 Y. Kodama, K. Nishihata, M. Nishio and Y. Iitaka, *J. Chem. Soc., Perkin Trans. 2*, 1976, 1490.
13 H. Okawa, *Coord. Chem. Rev*., 1988, **92**, 1.
14 M. Levitt and M. F. Perutz, *J. Mol. Biol*., 1988, **201**, 751.
15 M. Nishio and M. Hirota, *Tetrahedron*, 1989, **45**, 7201.
16 M. Nishio, Y. Umezawa, M. Hirota and Y. Takeuchi, *Tetrahedron*, 1995, **51**, 8665.
17 E. Fischer and H. Sigel, *J. Am. Chem. Soc*., 1980, **102**, 2998.
18 K. Kobayashi, Y. Asakawa, Y. Kikuchi, H. Toi and Y. Aoyama, *J. Am. Chem. Soc*., 1993, **115**, 2648.
19 K. Jitsukawa, K. Iwai, H. Masuda, H. Ogoshi and H. Einaga, *Chem. Lett*., 1994, 303.
20 D. M. Smith, N. R. Thomas and D. Gani, *Experimentia*, 1991, **47**, 1104.
21 A. M. Catherine, G. V. Michel and N. J. Johan, *J. Mol. Biol*., 1992, **225**, 495.
22 P. A. Clark, J. N. Jansonius and E. L. Mehler, *J. Am. Chem. Soc*., 1993, **115**, 1894.
23 P. A. Clark, J. N. Jansonius and E. L. Mehler, *J. Am. Chem. Soc*., 1993, **115**, 9790.
24 P. Christen and D. E. Metzler (Editors), *Transaminases*, Wiley, New York, 1985.
25 K. Dakshinamurti, *Ann. N.Y. Acad. Sci*., 1990, vol. 585.
26 J. Kielland, *J. Am. Chem. Soc*., 1973, **59**, 1675.
27 J. A. Ibers and W. C. Hamilton (Editors), *International Tables for X-Ray Crystallography*, Kynoch Press, Birmingham, 1974, vol. 4.
28 MOLEN, *An Interactive Structure Solution Procedure*, Enraf-Nonius, Delft, 1990.
29 J. E. Fergusson, *Stereochemistry and Bonding in Inorganic Chemistry*, Prentice-Hall, New York, 1974.
30 K. Jitsukawa, T. Yamamoto, H. Masuda and H. Einaga, unpublished work.
31 E. H. Abbott and A. E. Martell, *J. Am. Chem. Soc*., 1969, **91**, 6866.
32 E. H. Abbott and A. E. Martell, *J. Am. Chem. Soc*., 1970, **92**, 5845.
33 M. Noritake, K. Okamoto, J. Hidaka and H. Einaga, *Bull. Chem. Soc. Jpn*., 1990, **63**, 353.
34 R. J. Motekaitis, Y. Sun and A. E. Martell, *Inorg. Chim. Acta*, 1989, **159**, 29.
35 C. K. Johnson, ORTEP, Report ORNL-5138, Oak Ridge National Laboratory, Oak Ridge, TN, 1976.
36 L. Pauling, *The Nature of the Chemical Bond*, Cornell University Press, Ithaca, 3rd edn., NY, 1960.
37 C. E. Johnson and F. A. Bovey, *J. Chem. Phys*., 1958, **29**, 1012.
38 T. Yasui, J. Hidaka and Y. Shimura, *J. Am. Chem. Soc*., 1965, **87**, 2762.

Received 28*th April* 1997; *Paper* 7/02900D